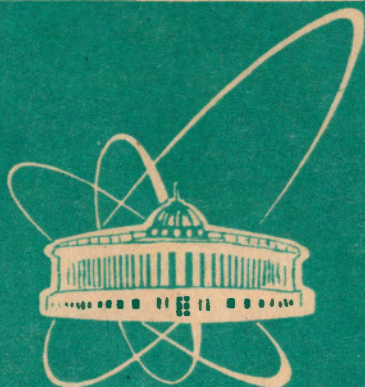


93-201



ОБЪЕДИНЕННЫЙ
ИНСТИТУТ
ЯДЕРНЫХ
ИССЛЕДОВАНИЙ
ДУБНА

E2-93-201

O.V.Bespalova¹, V.V.Burov, B.S.Galakhmatova¹,
H.G.Miller², E.A.Romanovsky¹, M.V.Rzjanin,
K.V.Shitikova¹, G.D.Yen²

**STRUCTURE OF THE NEUTRON-RICH
LITHIUM ISOTOPES
IN HEAVY-ION REACTIONS**

Submitted to «Zeitschrift für Physik A»

¹Institute of Nuclear Physics, Moscow State University, Moscow, Russia

²Department of Physics, University of Pretoria, Pretoria 0002, Republic of South Africa

1993

1 Introduction

In the past few years, the fragmentation of relativistic projectiles and the separation of the produced fragments offered the possibility to prepare high-quality beams of exotic nuclei. Experiments with these beams allowed for investigation of the properties of nuclei far from stability and their comparison to the results obtained with stable or less exotic beams. The first experiments [1, 2] mainly showed two surprising features. Firstly, the nuclear matter radii of these neutron-rich nuclei extracted from measured total interaction cross sections on targets with low nuclear charge Z are much larger than predicted by the scaling laws usually used [3]. Secondly, the interaction cross sections on high- Z targets are only understandable if it is assumed that electromagnetic dissociation plays an important role, i. e. is about 10 to 100 times larger than for stable nuclei of similar masses. It has been assumed that this effect is due to a low-lying giant resonance at about 1 MeV excitation energy [4].

In [5] presented were results on total charge-changing cross sections for the lithium isotopes $^8,9,11\text{Li}$ on different targets. The high-energy reaction cross sections of Li and Be isotopes are calculated using a simplified Glauber model and densities constrained by the empirical binding energies [6]. The electromagnetic dissociation in the (^{11}Li , ^9Li) projectile fragmentation has been studied using a formalism developed by Winther and Alder [7]. A large-scale shell-model calculation is applied to the study of radii of neutron-rich p-shell nuclei, using harmonic-oscillator and Hartree-Fock single-particle wave functions [8]. In [9] cross section measurements of the neutron-rich isotopes $^8,9,11\text{Li}$ were done at 80 MeV/nucleon. In [10] a unified calculation of neutron-rich isotopes in lithium has been performed in a hyperspherical basis in which the underlying symmetry of each isotope exhibits a simple structure. The variation in the binding energy as a function of mass number is qualitatively reproduced, and the radial distribution of each isotope decreases exponentially asymptotically. It is shown that the form factors for isotopes of $^6,7\text{Li}$ well agree with the experimental data at small moment transfer.

In the present paper we calculated in the unified way the properties of neutron-rich Li isotopes. This paper is organized as follows. The structure

properties of the neutron-rich Li isotopes are discussed in sect. 2. Sect. 3 is devoted to discussion on calculation results of the form factors and angular distributions of elastic scattering of neutron-rich lithium isotopes. In sect. 4 we calculate nuclear interaction cross section of Li neutron-rich isotopes basic concept of Carol's microscopic model. It is based on the Glauber theory and semiclassical optical model.

2 The Structure Properties of the Li Neutron-Rich Isotopes

Exotic nuclei close to the neutron drip line are difficult to describe microscopically. The small binding energies and extended radial density distributions of neutron-rich nuclei such as the lithium isotopes, which are produced in radioactive beams [1, 2, 4, 9], are not correctly reproduced in either Hartree-Fock or shell model calculations [6, 11]. For this reason simple Gaussian parameterizations of the density distributions [6] have been used in order to describe the large experimentally observed reaction cross sections [1, 2, 4].

In [10] a fully microscopic calculation of the lithium isotopes has been performed in a basis of hyperspherical functions with the symmetries properly

Table

${}^A\text{Li}$	$[f]$	J^π	L	S	T
6	[42]	1^+	0	1	0
7	[43]	$3/2^-$	1	1/2	1/2
8	[431]	2^+	2	0	1
9	[432]	$3/2^-$	1	1/2	3/2
11	[4322]	$3/2^-$	1	1/2	5/2

taken into account [12, 13]. In this basis a better description of the asymptotic part of the wave functions is possible. Unlike some previous theoretical treatments [7, 14], in [10] an attempt was done to provide a unified description of ${}^6,7,8,9,11\text{Li}$ rather than that of just a single isotope. No attempt will be made to parameterize the effective interaction used for each isotope, rather a simple parameterization for all the isotopes has been used. Furthermore in this treatment there is no inert core [7, 14] and all of the nucleons are properly antisymmetrized. Lastly because Jacobi coordinates were used, no problems are encountered with the treatment of the center of mass [8].

In order to provide a unified description of all of the lithium isotopes we use the following group theoretical description. In the Table the spin and isospin of each of the isotopes are given. From knowledge of the total isospin the symmetry of each isotope is determined. As can be seen from the table the corresponding Young diagram [f] for each isotope exhibits a simple structure. ${}^{11}\text{Li}$ is constructed from ${}^9\text{Li}$ plus two neutrons in the same manner as ${}^9\text{Li}$ from ${}^7\text{Li}$ plus two neutrons. Fig. 1 shows the convenient Young diagram for all the Li-rich isotopes.

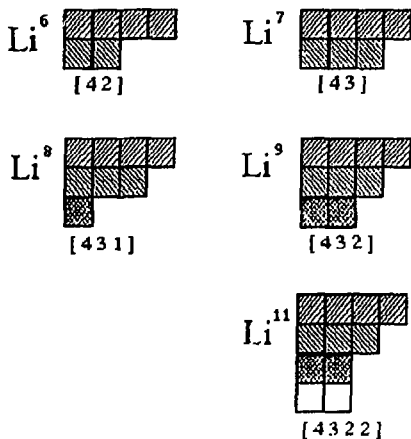


Figure 1: Young diagram for all Li-rich isotopes

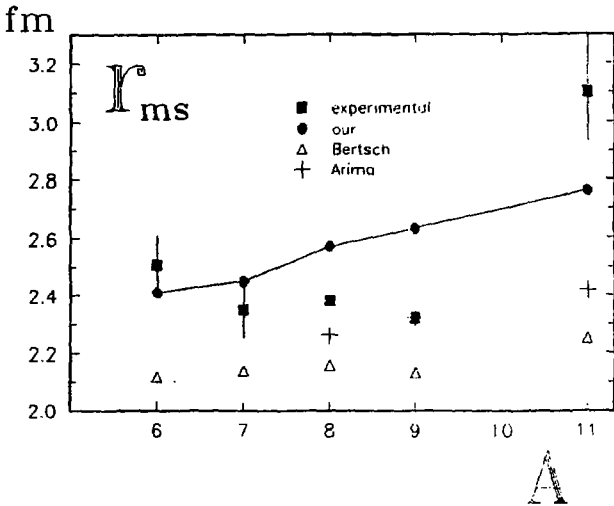


Figure 2: Mean squared radius of Li isotopes

In [10] the variation in the binding energy as a function of mass number is qualitatively reproduced, and the radial distribution of each isotope decreases exponentially asymptotically. Fig. 2 shows the calculation results from [10] of the mean squared radius of Li as a function of mass number in comparison with experimental data and calculation results from [6, 8]. It is seen that all the calculation results are much smaller than the experimental value 3.10 ± 0.17 fm for ^{11}Li , but our calculation results are bigger than the others.

3 The Form Factors and Angular Distributions of Elastic Scattering of Neutron-Rich Li Isotopes

With the radial density distributions of the isotopes of lithium from [10] we have calculated the form factors and cross sections of the angular distributions of elastic scattering on ^{12}C . The expression for the elastic and inelastic form factors in the high energy approximation [15] has the form:

$$F_{ij} = 2\pi i q \sum_{\epsilon=\pm 1} \int_0^{\infty} \frac{G_{ij}(x, \epsilon)}{\tilde{q}^2(x, \epsilon)} e^{x\rho\{i[qR\epsilon + \Phi(x, \epsilon)]\}} n_{ij}(x) x dx. \quad (1)$$

where the functions G , \tilde{q} , Φ take into account the distortion of electron wave with the Coulomb field of nucleus (see [15]). In the Born approximation $G = 1$, $\Phi = 0$, $\tilde{q} = q$. The formula (1) is correct for $qR \gg 1$, $V(0)/E \ll 1$, $E^* < E$, where $V(0)$ - the Coulomb potential in the center of nucleus, E^* - loss of the energy of the electron.

Elastic $^6\text{Li}+^{12}\text{C}$ and $^{11}\text{Li}+^{12}\text{C}$ differential cross section are analyzed within the framework of the standard double-folding model [16] for the real part of the optical potential, using standard DDM3Y effective nucleon-nucleon interactions [17] and Wood-Saxon imaginary potential. Real optical potential is given by

$$U(\vec{R}) = N \int d\vec{r}_1 d\vec{r}_2 \rho_1^m(\vec{r}_1) \rho_2^n(\vec{r}_2) V(\vec{r}_{12} = \vec{R} + \vec{r}_2 - \vec{r}_1), \quad (2)$$

where N is the overall potential normalization factor, ρ_1^m (ρ_2^n) are the density distributions of the projectile (target) nuclei, and $V(r)$ is effective interaction. Figs. 3 - 6 show our calculation results of ^6Li and ^{11}Li form factors and cross sections of $^6\text{Li}+^{12}\text{C}$ and $^{11}\text{Li}+^{12}\text{C}$ elastic scattering. Fig. 3 gives the calculation results of the form factors for ^6Li in comparison with the experimental data. Fig. 5 presents the calculation results of the form factors of ^{11}Li in comparison with the calculation results with the density distribution from [6]. Fig. 4 and Fig. 6 show the calculated results and experimental data for the scattering $^6\text{Li}+^{12}\text{C}$ at $E_{lab}(^6\text{Li})=210$ MeV and $^{11}\text{Li}+^{12}\text{C}$ at $E_{lab}(^{11}\text{Li})=637$ MeV, respectively. The density [10] was used for ^6Li and ^{11}Li while the used ^{12}C

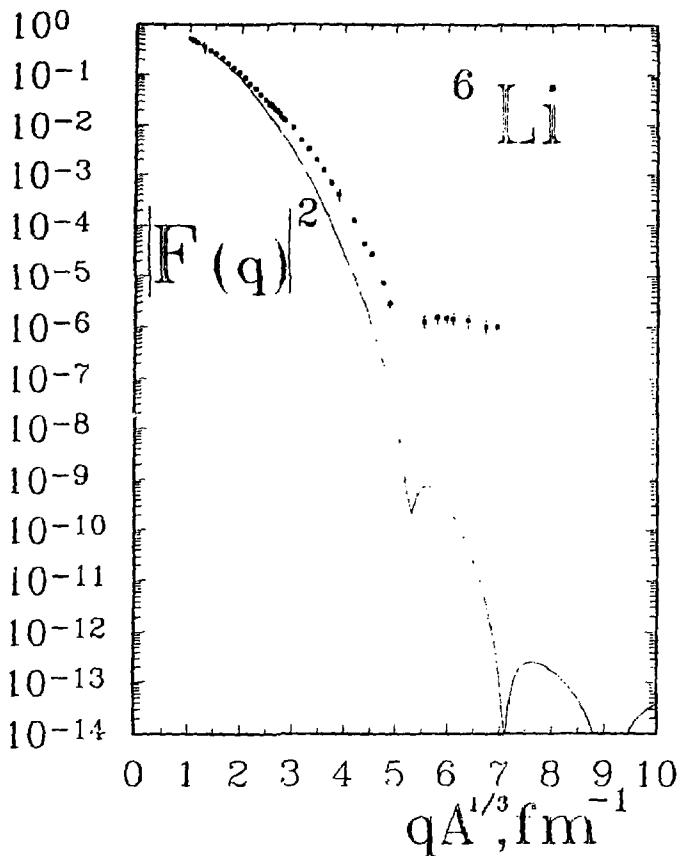


Figure 3: Form factor of ${}^6\text{Li}$

density distribution was that obtained from elastic electron scattering. A three-parameter Fermi distribution [18] is

$$\rho^m(r) = \frac{\rho_0(1 + \omega r^2/c^2)}{1 + \exp[(r-c)/z]} \quad (3)$$

with $c = 2.355$ fm, $\omega = -0.149$, $z = 0.5224$.

The normalization of the real double-folding potential N and the three

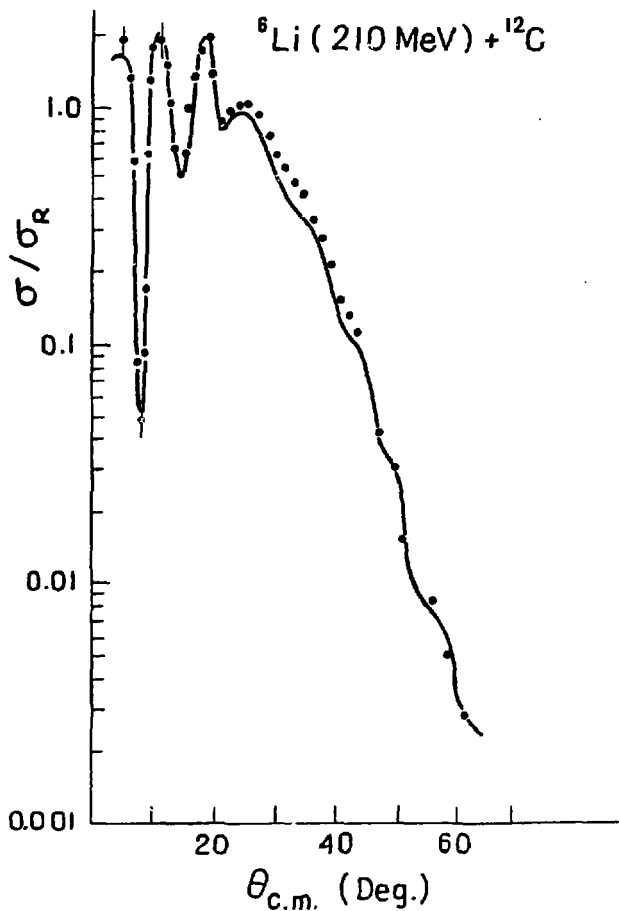


Figure 4: The angular distribution of elastic ${}^6\text{Li} + {}^{12}\text{C}$ scattering at 210 MeV

variables of the imaginary potential W , r , a were varied to obtain the optimal fit to the data. The criterion of fitting is the usual one, namely we minimized

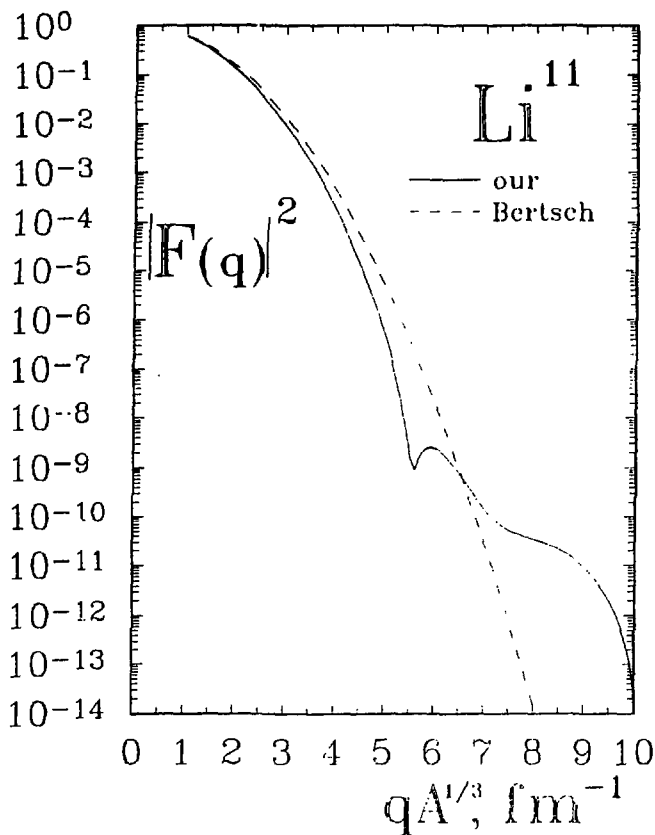


Figure 5: Form factors of ^{11}Li : solid line is our result, dashed line is result with Bertsch's density distributions

the value:

$$\chi^2 = \sum (\sigma_{exp}(\Theta_i) - \sigma_{theor}(\Theta_i))^2 / (\Delta\sigma_{exp}(\Theta_i))^2. \quad (4)$$

A charge radius parameter $r = 1.3$ was used for the Coulomb potential.

Our analysis of the 210 MeV $^6\text{Li} + ^{12}\text{C}$ elastic scattering yields for the normalization of double folded potential a value 0.8. The value of the real

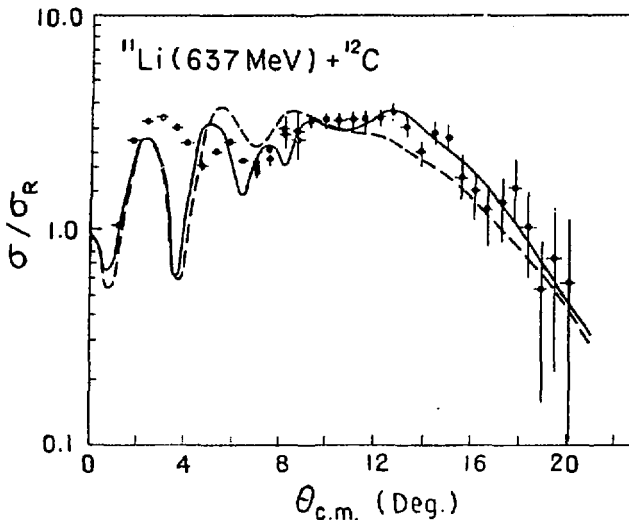


Figure 6: The angular distribution of elastic $^{11}\text{Li}+^{12}\text{C}$ scattering

volume integral $J_r/A_t A_p$ obtained in our calculations is $\sim 260 \text{ MeV}\cdot\text{fm}^3$ and the value of the imaginary volume integral $J_i/A_t A_p$ is $180 \text{ MeV}\cdot\text{fm}^3$. The values of the volume integrals $J_r/A_t A_p$ and $J_i/A_t A_p$ calculated according to the equations given by Gupta et al. [19] are $300 \text{ MeV}\cdot\text{fm}^3$ and $140 \text{ MeV}\cdot\text{fm}^3$, correspondingly. The total cross section of the reaction from our analysis is 1011 mb . This is in a good agreement with results of the simple optical model [20], where there were obtained the values $J_r/A_t A_p = 298, 401 \text{ MeV}\cdot\text{fm}^3$, $J_i/A_t A_p = 160, 166 \text{ MeV}\cdot\text{fm}^3$, and $\sigma_{tot} = 1105 \text{ mb}$ for different sets of parameters. In the paper [21] the first double folded analysis of the $210 \text{ MeV } ^6\text{Li} + ^{12}\text{C}$ elastic scattering was carried out and a value of the normalization of the double folded potential was found 0.57 ; and the value of the imaginary volume integral was found $\sim 170 \text{ MeV}\cdot\text{fm}^3$.

Kolata et al. [22] have measured the elastic scattering at 60 MeV/nucleon of the exotic halo nucleus ^{11}Li on a ^{12}C target and have carried out analysis of this scattering. Angular distribution for the elastic scattering of ^{11}Li from

^{12}C is shown in Fig. 6. The horizontal error bars indicate the averaging interval of the experimental data due to the angular resolution of the detection system including multiple scattering. The vertical error bars are purely statistical. The calculations were carried in the framework of different models. The best agreement with experiment is achieved by calculating the $^{11}\text{Li} + ^{12}\text{C}$ elastic scattering in the framework of the coupled-channels method and adding inelastic cross section for the excitation of the lowest 2^+ and 3^- states in ^{12}C which should make the largest contributions. The result of this calculation is shown by a dashed curve in Fig. 6. The large discrepancy in the region of 4 remains unexplained. The total reaction cross section resulting from the coupled-channels calculation is 1350 mb. The systematics [23] of ^{11}Li interaction cross section measurements predicts a value closer to 1600 mb. Satchler et al. [24] have shown that introduction of long-range absorption due to the fragmentation from the halo can increase the reaction cross section by several hundred mb with negligible effect on the predicted angular distribution.

Our calculation carried out within the framework of the standard optical model gives the description of the $^{11}\text{Li} + ^{12}\text{C}$ elastic scattering comparable with the results of [22] (solid curve in Fig. 6). Our results yield a value 1.15 for the normalization of the double folded potential. The total reaction cross section resulting from our calculations is 1613 mb which is in agreement with [23].

4 Nuclear Interaction Cross Section of Neutron-Rich Lithium Isotopes

One of the most fundamental quantities characterizing the nuclear structure in the heavy ions reactions is the total reaction cross section σ_r . This quantity has been studied both theoretically and experimentally for various systems particle+nucleus. Recently a possibility has appeared to measure σ_r for unstable neutron-rich nuclei for the sake of determining its sizes

In this paper we will present a calculation of the σ_r for Li isotopes scattering on ^{12}C at 80 and 790 MeV per nucleon. Here we use approximation to

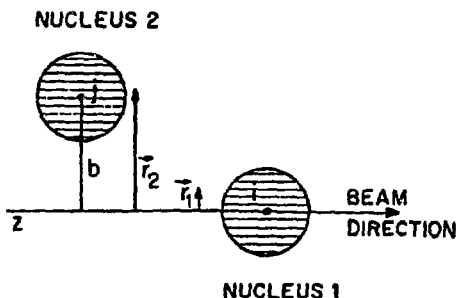


Figure 7: Diagrammatic representation of the nucleus-nucleus collision. Each nucleus is divided into tubes denoted by i and j . The value b is the impact parameter

the Glauber model based on the individual nucleon-nucleon collisions in the overlap volume of the colliding nuclei to calculate σ_r [25, 26].

In the absence of the Coulomb field for a zero-range interaction the nucleus-nucleus reaction cross section in the framework of approximation to the Glauber model can be written as

$$\sigma_r = 2\pi \int b db [1 - \exp[-\overline{\sigma_{NN}} \int d^2r_1 \rho_z^1(\vec{r}_1) \rho_z^2(|\vec{r}_1 - \vec{b}|)]], \quad (5)$$

where $\overline{\sigma_{NN}}$ is the nucleon-nucleon reaction cross section averaged over the interacting n-n, p-p and n-p pairs, \vec{b} is the impact parameter, \vec{r}_1 is shown in Fig 7. The thickness function $\rho_z^i(\vec{r}_1)$ is defined by

$$\rho_z^i(\vec{r}) = \int_{-\infty}^{\infty} dz \rho^i(r^2 + z^2)^{\frac{1}{2}} \quad (i = 1, 2), \quad (6)$$

where ρ^i is the nuclear density and z is the beam direction. The expression (5) is derived by neglecting the transverse motion while the nuclei pass each other.

As the model was first developed for the relativistic energy range, straight-line trajectories were assumed for the projectile in Equation (5). In our calculation we have included deflection of the projectile due to the Coulomb repulsion, which can be important at subrelativistic energies. At first order correction

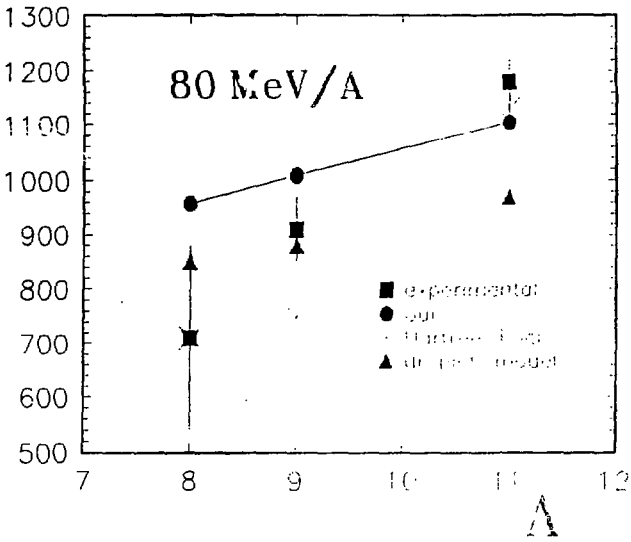
$\sigma_{\text{tot}}, \text{mb}$ 

Figure 8: Total cross section for Li isotopes on ^{12}C target at 80 MeV/nucleon: our results, experimental data and Blank's theoretical results

Coulomb effect can be taken into account by replacing $\rho_z^2(|\vec{r}_1 - \vec{b}|)$ by $\rho_z^2(|\vec{r}_1 - \vec{b}'|)$ [26], where b' is the classical distance of the closest approach of the projectile in the Coulomb potential.

The projectile and target density distributions are very important in microscopic calculation σ_r . We used density Li isotopes [10] and density of ^{12}C obtained from the electron scattering data [27].

Quantities $\overline{\sigma_{nn}}$ were calculated using expressions from [29]

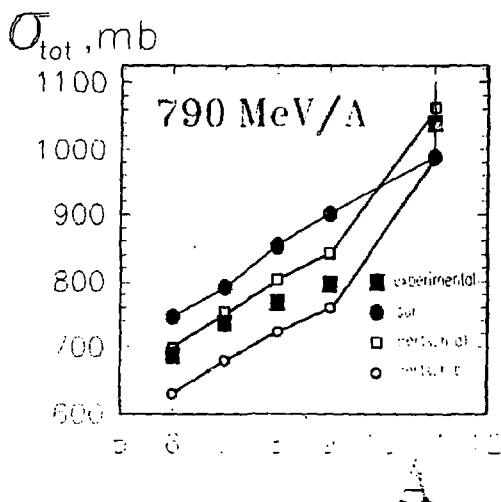


Figure 9: Total cross section for Li isotopes on ^{12}C target at 790 MeV/nucleon

$$\overline{\sigma_{NN}} = (N_p N_l \sigma_{nn} + Z_p Z_l \sigma_{pp} + N_p Z_l \sigma_{np} + N_l Z_p \sigma_{np}) / (A_p A_l)$$

$$\sigma_{np} = -70.67 - 18.18/\beta + 25.26/\beta^2 + 113.85\beta (\text{mb}). \quad (7)$$

$$\sigma_{pp} = \sigma_{nn} = 13.73 - 15.04/\beta + 8.76/\beta^2 + 68.67\beta^3 (\text{mb}).$$

where $\beta = v/c$.

The reaction cross sections of Li isotopes on ^{12}C target at 80 and 790 MeV per nucleon calculated numerically are shown in Figs. 8,9 in comparison with the experimental data from [6, 28]. It can be seen that the reaction cross sections of ^{11}Li on ^{12}C target agree with experimental data quite well. In the case of $^{6,7,8,9}\text{Li} + ^{12}\text{C}$ our calculation results overestimate experimental data for both energies 80 and 790 MeV/nucleon.

Note that in the case of 790 MeV per nucleon experimental data for interaction cross sections σ_I were used instead of σ_r . σ_I is a part of the total reaction cross section. Evaluation of σ_r greater than σ_I by about 5% has been

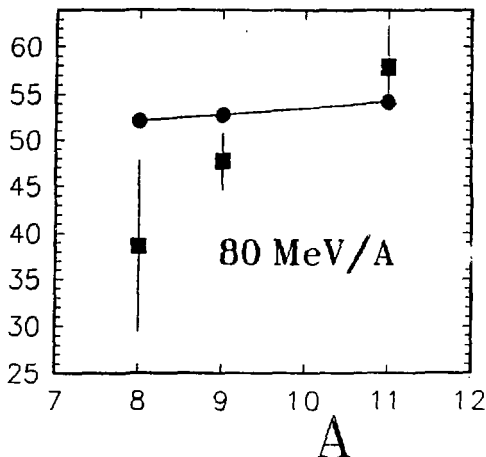
$\pi R^2, \text{mb}$ 

Figure 10: Square of the radius parameter for Lithium at 80 MeV/nucleon. Boxes are experimental data, circles are our calculation results

made in [16].

The total reaction cross section can be represented in a simple form

$$\sigma_r = \pi r_0^2 (A_p^{1/3} + A_t^{1/3})^2 (1 - V_c/E_{c.m.}), \quad (8)$$

here r_0 - interaction radius parameter, V_c - Coulomb barrier

$$V_c = (1.44 Z_p Z_t) / (A_p^{1/3} + A_t^{1/3}). \quad (9)$$

The increase of r_0 with increasing neutron excess of the nucleus is the so-called isotopic effect in the total reaction cross section. This effect is observed for protons, deuterons, α -particles and heavy ion scattering on neutron-rich targets. In the framework of approximation to the Glauber model, isotopic

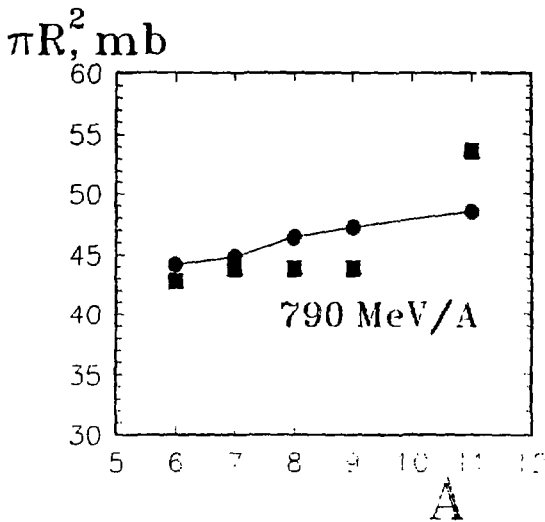


Figure 11: Square of the radius parameter for Lithium at 790 MeV/nucleon. Boxes are experimental data, circles are our calculation results

effects result from dependence of neutron distribution diffuseness on neutron excess [30]. We have converted the calculated and the experimental σ_r into r_0^2 according to Eq.(8). Dependencies of πr_0^2 on mass number of Li isotopes presented in Fig. 10 and Fig. 11 show that the calculated πr_0^2 increases linearly with increasing A_p . This is in accordance with experimental results for various systems projectile+target (see [30]).

5 Conclusion

We have calculated in the unified way the properties of neutron-rich Li isotopes. We have studied the structure properties of the neutron-rich Li isotopes, form factors and angular distributions of elastic scattering of neutron-rich lithium isotopes. We have calculated nuclear interaction cross section of Li neutron-rich isotopes based on the Glauber theory and semiclassical optical model. We have compared the calculation results with the experimental data and calculation results from other theoretical approaches. A good qualitative agreement has been obtained for describing the nuclear structure and the scattering properties.

References

- [1] Tanihata, I., Hamagaki, H., Hashimoto, O., Nagamiya, S., Shida, Y., Yoshikawa, N., Yamakawa, O., Sugimoto, K., Kobayashi, T., Greiner, D.E., Takahashi, N., Nojiri, Y.: Phys. Lett. B **160**, 380 (1985)
- [2] Tanihata, I., Hamagaki, H., Hashimoto, O., Shida, Y., Yoshikawa, N., Sugimoto, K., Yamakawa, O., Kobayashi, T., Takahashi, N.: Phys. Rev. Lett. **55**, 2676 (1985)
- [3] Tanihata, I., Kobayashi, T., Yamakawa, O., Shimoura, S., Ekuni, K., Sugimoto, K., Takahashi, N., Shimoda, T., Suto, H.: Phys. Lett. B **206**, 592 (1988)
- [4] Kobayashi, T., Yamakawa, O., Omata, K., Sugimoto, K., Shimoda, T., Takahashi, N., Tanihata, I.: Phys. Rev. Lett. **60**, 2599 (1988)
- [5] Blank, B. et al.: "Charge-changing cross sections of the neutron-rich isotopes $^8,9,11\text{Li}$ " GSI-92-22 (march 1992)
- [6] Bertsch, G.F., Brown, B.A., Sagawa, H.: Phys. Rev. C **39**, 1154 (1989)
- [7] Suzuki, Y., Tosaka, Y.: Nucl. Phys. A **517**, 599 (1990)
- [8] Hoshino, T., Sagawa, H., Arima, A.: Nucl. Phys. A **506**, 271 (1990)

- [9] Blank, B., Gaimard, J.J., Geissel, H., Schmidt, K.H., Stelzer, H., Sümmerer, K., Bazin, D., Del Moral, R., Dufour, J.P., Fleury, A., Hubert, F., Clerc, H.G., Steiner, M.: *Z. Phys. A* **340**, 41 (1991)
- [10] Burov, V.V. et al.: *JINR Preprint, Dubna E2-93-41* (1993)
- [11] Sato, H., Okuhara, Y.: *Phys. Lett. B* **162**, 217 (1985)
- [12] Smirnov, Y.F., Shitikova, K.V.: *Particles and Nucleus* **8**, 847 (1977)
- [13] Shitikova, K.V.: *Nucl. Phys. A* **331**, 365 (1979)
- [14] Bertsch, G.F., Esbensen, H.: *Ann. Phys.* **209**, 327 (1991)
- [15] Lukyanov, V.K., Pol', Yu.S.: *Particles and Nucleus* **5**, 955 (1974)
- [16] Satchler, G., Love, W.: *Phys. Rep.* **55**, 183 (1979)
- [17] El-Azab Farid, M., Satchler, G.: *Nucl. Phys. A* **438**, 525 (1985)
- [18] Suelze, L.R., Yearian, M.Y., Cramel, H.: *Phys. Rev.* **162**, 992 (1967)
- [19] Gupta, S.K., Kailas, S., Lingappa, N., Shridhar, A.: *Phys. Rev. C* **31**, 1965 (1985)
- [20] Nadasen, A. et al.: *Phys. Rev. C* **37**, 132 (1988)
- [21] Trecka, D.E., Frawley, A.D., Kemper, K.W., Robson, D., Fox, J.D., Meyers, E.G.: *Phys. Rev. C* **41**, 2134 (1990)
- [22] Kolata, J.J. et al.: "Elastic scattering of ^{11}Li and ^{11}C from ^{12}C at 60 MeV/nucleon" preprint MSU (1992)
- [23] Yabana, K. et al.: *Nucl. Phys. A* **539**, 295 (1992)
- [24] Satchler, G.W., McVoy, K.W., Hussein, M.S.: *Nucl. Phys. A* **522**, 621 (1991)
- [25] Karol, P.J.: *Phys. Rev. C* **11**, 1203 (1975)
- [26] Devries, R.M., Peng, J.C.: *Phys. Rev. C* **22**, 1055 (1980)

- [27] Jager, C.W., De Vries, H., De Vries, C.: Atomic Data and Nuclear Data. Tables **14**, 479 (1974)
- [28] Blank, B. et al.: "Total and $2n$ -removal cross sections of the neutron-rich isotopes $^8,9,11\text{Li}$ " **GSI-92-41** (june 1992)
- [29] Charogi, S.K., Gupta, S.K.: Phys. Rev. C **41**, 1610 (1990)
- [30] Shen, W., Wang, B., Feng, J., Zhou, W., Zhu, Y., Feng E.: Nucl. Phys. A **491**, 130 (1989)

**Received by Publishing Department
on June 2, 1993.**